

An Improved Measurement of Electroweak Couplings from $e^+ e^- \rightarrow e^+ e^-$ and $e^+ e^- \rightarrow \mu^+ \mu^-$

TASSO Collaboration

M. Althoff, W. Braunschweig, F.J. Kirschfink,
K. Lübelmeyer, H.-U. Martyn, G. Peise, J. Rimkus,
P. Roskamp, H.G. Sander, D. Schmitz, H. Siebke,
W. Wallraff

I. Physikalisches Institut der RWTH,
D-5100 Aachen, Federal Republic of Germany^a

H.M. Fischer, H. Hartmann, W. Hillen¹, A. Jocksch,
G. Knop, L. Köpke, H. Kolanoski, H. Kück,
R. Wedemeyer, N. Wermes², M. Wollstadt³

Physikalisches Institut der Universität,
D-5300 Bonn, Federal Republic of Germany^a

H. Burkhardt⁴, Y. Eisenberg⁵, K. Gather,
H. Hultschig, P. Joos, W. Koch, U. Kötz,
H. Kowalski, A. Ladage, B. Löhr, D. Lüke, P. Mättig,
D. Notz, J. Pyrlík, D.R. Quarrie⁶, M. Rushton,
W. Schütte, D. Trines, G. Wolf, Ch. Xiao

Deutsches Elektronen-Synchrotron, DESY,
D-2000 Hamburg, Federal Republic of Germany

R. Fohrmann, E. Hilger, T. Kracht, H.L. Krasemann,
P. Leu, E. Lohrmann, D. Pandoulas, G. Poelz,
B.H. Wiik

II. Institut für Experimentalphysik der Universität,
D-2000 Hamburg, Federal Republic of Germany^a

R. Beuselinck, D.M. Binnie, A.J. Campbell,
P.J. Dornan, B. Foster, D.A. Garbutt, C. Jenkins,

T.D. Jones, W.G. Jones, J.McCardle, J.K. Sedgbeer,
W.A.T. Wan Abdullah

Department of Physics, Imperial College,
London SW7 2BZ, England^b

K.W. Bell, M.G. Bowler, I.C. Brock⁷, R.J. Cashmore,
P.E.L. Clarke, R. Devenish, P. Grossmann, S.L. Llyod,
G.L. Salmon, J. Thomas, T.R. Wyatt, C. Youngman

Department of Nuclear Physics,
University, Oxford OX1 3RH, England^b

J.C. Hart, J. Harvey, D.K. Hasell, J. Proudfoot,
D.H. Saxon, P.L. Woodworth⁸

Rutherford Appleton Laboratory, Chilton,
Didcot, Oxon OX11 0QX, England^b

F. Barreiro, M. Dittmar, M. Holder, B. Neumann
Fachbereich Physik der Universität-Gesamthochschule,
D-5900 Siegen, Federal Republic of Germany^a

E. Duchovni, U. Karshon, G. Mikenberg, R. Mir,
D. Revel, E. Ronat, A. Shapira, G. Yekutieli
Weizmann Institute, Rehovot, Israel^c

T. Barklow, A. Caldwell, M. Cherney, J.M. Izen,
M. Mermikides, G. Rudolph, D. Strom,
H. Venkataramania, E. Wicklund, Sau Lan Wu,
G. Zobernig

Department of Physics, University of Wisconsin,
Madison, WI 53706, USA^d

Received 30 September 1983

Abstract. We present an analysis of electroweak leptonic couplings from high statistics experiments on Bhabha scattering and μ pair production at an energy of 34.5 GeV. The forward-backward charge

asymmetry of the μ pairs was measured to be $-0.098 \pm 0.023 \pm 0.005$. The data were found to agree well with the standard theory of electroweak interaction giving $\sin^2 \theta_w = 0.27 \pm 0.07$. The leptonic

¹ Now at Philips, Aachen, FRG

² Now at SLAC, Stanford, CA., USA

³ Now at Lufthansa, Frankfurt, FRG

⁴ Now at CERN, Geneva, Switzerland

⁵ On leave from Weizmann Institute, Rehovot, Israel

⁶ Now at FNAL, Batavia, USA

⁷ Now at Carnegie-Mellon University, Pittsburg, USA

⁸ Now at Institute of Oceanographic Sciences, Bidston, Merseyside, UK

^a Supported by the Deutsches Bundesministerium für Forschung und Technologie

^b Supported by the UK Science and Engineering Research Council

^c Supported by the Minerva Gesellschaft für Forschung mbH

^d Supported by the US Department of Energy contract WY-76-C-02-0881

weak couplings were determined to be $g_V = 0.000 \pm 0.170$ and $g_A = -0.481 \pm 0.055$. The data were also used to investigate a class of composite models for leptons.

In this paper we present a new analysis of the leptonic reactions

$$e^+ e^- \rightarrow e^+ e^- \quad (1)$$

and

$$e^+ e^- \rightarrow \mu^+ \mu^- \quad (2)$$

at an average c.m. energy of $W = 34.5$ GeV based on an integrated luminosity of 74.7 pb^{-1} .

With the high statistics available we performed tests of QED and studied electroweak interference effects. The most prominent observation is a significant charge asymmetry in the μ pair production, which is in accordance with the Glashow-Weinberg-Salam (GWS) prediction [1]. From a combined fit to both reactions the electroweak coupling constants were determined. We also used the data to set limits on possible extensions of the standard theory. The data were compared with the neutral current predictions given by the following lagrangian [2]:

$$L_{\text{eff}}^{\text{NC}} = \frac{4 G_F}{\sqrt{2}} \{ (j^{(3)} - \sin^2 \theta_W \cdot j_{\text{em}})^2 + c \cdot j_{\text{em}}^2 \}. \quad (3)$$

Here G_F is the Fermi constant, $j^{(3)}$ the third component of the weak isospin current, j_{em} the electromagnetic current and θ_W the Weinberg angle. The parameter c is identically zero in $SU(2) \times U(1)$ models such as that of GWS. Alternatives to the standard theory [2, 3], e.g. models with extended gauge groups, supersymmetry or composite fermions and gauge bosons can lead to $c > 0$. The strength of the weak interaction is expressed by dimensionless vector and axial vector coupling constants g_V^l and g_A^l ($l = e, \mu$), respectively:

$$g_V = \sqrt{\rho} (I_{3L} + I_{3R} + 2 \sin^2 \theta_W) \quad (4)$$

$$g_A = \sqrt{\rho} (I_{3L} - I_{3R}). \quad (5)$$

I_{3L} and I_{3R} are the third components of the left-handed and right-handed weak isospins of the leptons and the parameter ρ is related to the number of Higgs particles. In the standard theory, which is strongly supported by neutrino and electron deuteron scattering experiments [4], by $e^+ e^-$ annihilation experiments at PETRA and PEP [5-7], and by the recent discoveries of the W and Z bosons [8, 9], $I_L = \frac{1}{2}$, $I_R = 0$, $\rho = 1$ and $\sin^2 \theta_W$ is the only free

parameter. Of particular interest is a comparison of purely leptonic reactions from $e^+ e^-$ lepton production and neutrino electron scattering experiments. The analysis of νe experiments [4] has yielded $\sin^2 \theta_W = 0.23 \pm 0.04$ in the frame work of the GWS theory, or $g_V^e = -0.030 \pm 0.077$ and $g_A^e = -0.514 \pm 0.058$ in a 2 parameter model (the other solution allowed by νe scattering is excluded by data from $e^+ e^- \rightarrow l^+ l^-$ experiments).

The data were taken with the TASSO detector at the PETRA storage ring. The experiment, the trigger, the data taking and the analysis procedure were described previously [5, 6]. Results from part of the data (65 % of reaction (1) and 40 % of reaction (2)) were given in [6] and [5], respectively. In this paper we use exactly the same methods as before and more details can be found in the above references and the appendix. It is worth noting that charge dependent angular asymmetries due to the trigger and the track reconstruction are estimated to be less than 0.1 %.

We first discuss the analysis of Bhabha scattering events, followed by the analysis of μ pair production and then present a combined analysis of both reactions. The weak parameters were investigated in the following ways:

(i) determination of $\sin^2 \theta_W$ within the GWS theory,

(ii) determination of g_V^l and g_A^l assuming $M_Z = 95 \text{ GeV}^*$,

(iii) determination of the parameter c assuming $\sin^2 \theta_W = 0.23$.

Finally we investigate some tests of composite models.

$$e^+ e^- \rightarrow e^+ e^-$$

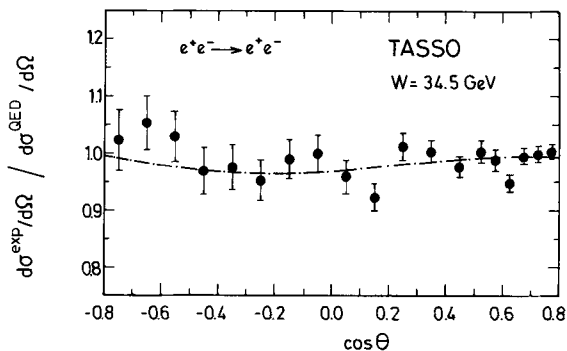
Bhabha scattering is of particular interest since the initial and final states contain the same leptons and therefore the assumption of lepton universality is not required. However, large contributions from one photon t -channel exchange induce a large positive forward-backward charge asymmetry. The sensitivity to the observation of new phenomena beyond QED is enhanced in the backward hemisphere.

The data sample contains 73801 Bhabha scattering candidates within the polar angle acceptance of $|\cos \theta| < 0.80$. The extraction of Bhabha scattering events is based solely on event topologies. Electrons and positrons were not positively identified. The

* For the Z mass we use a value consistent with the measurements of [9]. The results are not sensitive to the exact value of M_Z

Table 1. Cross section of $e^+e^- \rightarrow e^+e^-$ at $W=34.5$ GeV. The errors include statistical and systematic uncertainties apart from an overall normalization of $\pm 4.5\%$

$\langle \cos \theta \rangle$	$s \cdot d\sigma/d\Omega$ (GeV ² · nb/sterad)	$\sigma^{\text{meas}}/\sigma^{\text{QED}}$
0.775	$1,332.70 \pm 16.14$	1.004 ± 0.012
0.725	851.80 ± 11.04	1.000 ± 0.013
0.675	583.60 ± 8.10	0.996 ± 0.014
0.625	402.00 ± 6.52	0.949 ± 0.015
0.575	314.80 ± 5.58	0.989 ± 0.018
0.525	247.50 ± 4.78	1.004 ± 0.019
0.450	171.80 ± 2.95	0.977 ± 0.017
0.350	120.10 ± 2.31	1.004 ± 0.019
0.250	87.59 ± 1.95	1.014 ± 0.023
0.150	60.48 ± 1.58	0.923 ± 0.024
0.050	49.67 ± 1.44	0.959 ± 0.028
-0.050	42.37 ± 1.31	1.000 ± 0.031
-0.150	35.47 ± 1.20	0.990 ± 0.034
-0.250	29.64 ± 1.10	0.952 ± 0.035
-0.350	27.06 ± 1.08	0.975 ± 0.039
-0.450	24.50 ± 1.03	0.968 ± 0.041
-0.550	24.21 ± 1.04	1.028 ± 0.044
-0.650	23.48 ± 1.05	1.053 ± 0.047
-0.750	21.97 ± 1.15	1.022 ± 0.054

**Fig. 1.** The differential cross section divided by the QED expectation for the reaction $e^+e^- \rightarrow e^+e^-$. The curve shows the fit to the data of the GWS theory with $\sin^2 \theta_w = 0.27$

contributions from μ pairs ($\sim 5\%$) and τ pairs ($\sim 1\%$) were subtracted on a statistical basis. The data were corrected for detector losses and QED radiative effects to order α^3 for the photon exchange diagrams [10] by use of a Monte Carlo program. Contributions from radiative corrections to Z^0 exchange and higher order weak diagrams have not yet been calculated in a form applicable to experiments. They are expected to be small at PETRA energies. Systematic uncertainties in the acceptance as a function of the polar angle θ were less than 1% and were added in quadrature to the statistical errors. For cross section determinations the systematic errors amounted to $\pm 3.5\%$ for the overall corrections

and $\pm 4.5\%$ for the luminosity measurement derived from small angle Bhabha scattering.

Values of the differential cross section are listed in Table 1. In Fig. 1 we show the differential cross section as function of $\cos \theta$ divided by the QED prediction based on the luminosity measurement. The data are in excellent agreement with QED (see Table 2a). Traditionally any departure from QED has been parametrized by inserting time-like and space-like form factors,

$$F_T(s) = 1 \mp \frac{s}{s - \Lambda_{\pm}^2} \quad (6)$$

$$F_S(t) = 1 \mp \frac{t}{t - \Lambda_{\pm}^2}, \quad (7)$$

where $s = W^2$ and $t = -\frac{s}{2}(1 - \cos \theta)$. Lower limits on the cut off parameters Λ_{\pm} are given in Table 2a.

Although there is no evidence for deviations from QED, e.g. through electro-weak interference effects, the precision of the data allows one to put limits on the values of the weak parameters. The results of fits to the different assumptions (i)–(iii) above are listed in Table 2a. Within the GWS theory we obtain $\sin^2 \theta_w = 0.28^{+0.10}_{-0.14}$. This result is consistent with that obtained from neutrino electron scattering experiments. Note that in Bhabha scattering the values obtained for the electroweak couplings g_V^2 and g_A^2 are strongly correlated due to the t -channel exchange diagrams.

Table 2a. Results on QED and electroweak parameters from the reactions $e^+e^- \rightarrow e^+e^-$ and $e^+e^- \rightarrow \mu^+\mu^-$ at an average energy $W=34.5$ GeV. Where two errors are quoted, the first gives the statistical, the second the systematic uncertainty. Otherwise the error given includes both uncertainties

	$e^+e^- \rightarrow e^+e^-$	$e^+e^- \rightarrow \mu^+\mu^-$	Combined analysis
$\sigma^{\text{meas}}/\sigma^{\text{QED}}$	0.985 ± 0.013 ± 0.045	1.002 ± 0.020 ± 0.035	–
$\Lambda_{\pm}^{\text{QED}}$ (95% lower limit)	> 155 GeV	> 222 GeV	–
$\Lambda_{\pm}^{\text{QED}}$ (95% lower limit)	> 251 GeV	> 187 GeV	–
$\sin^2 \theta_w$	$0.28^{+0.10}_{-0.14}$	0.26 ± 0.10	0.27 ± 0.07
g_V^2	-0.15 ± 0.14	-0.01 ± 0.09	-0.034 ± 0.052
g_A^2	0.01 ± 0.16	0.27 ± 0.06	0.220 ± 0.054
g_V	–	–	0.000 ± 0.170
g_A	–	–	-0.481 ± 0.055
c	-0.010 ± 0.025	-0.002 ± 0.020	-0.009 ± 0.013
95% upper limit on c	< 0.032	< 0.029	< 0.013

Table 2b. Comparison of electroweak parameters from different experiments [7]. Where two errors are quoted, the first gives the statistical, the second the systematic uncertainty. Otherwise the error given includes both uncertainties

Experiment	W (GeV)	$A_{\mu\mu}$	g_A^2	g_V^2	$\sin^2\theta_W$
CELLO ^a	34.2	-0.064 ± 0.064	0.17 ± 0.17	-	0.25 ± 0.13
JADE ^b	33.5	$-0.128 \pm 0.038 \pm 0.01$	0.36 ± 0.11	0.05 ± 0.08	$0.26^{+0.12}_{-0.14}$
MARK J ^c	34.6	$-0.106 \pm 0.023 \pm 0.01$	$0.28 \pm 0.06 \pm 0.03$	$0.01 \pm 0.05 \pm 0.06$	0.24 ± 0.11
PLUTO ^d	34.7	$-0.134 \pm 0.031 \pm 0.01$	0.35 ± 0.08	-	-
MAC ^d	29.0	$-0.079 \pm 0.018 \pm 0.003$	0.31 ± 0.08	0.03 ± 0.16	-
TASSO ^e	34.5	$-0.098 \pm 0.023 \pm 0.005$	0.220 ± 0.054	-0.034 ± 0.052	0.27 ± 0.07

^a QED radiative corrections for μ pairs include only γ exchange diagrams. Values for g_A^2 from $\mu^+\mu^-$ pair data and for $\sin^2\theta_W$ from e^+e^- pair data

^b QED radiative corrections for μ pairs include only γ exchange diagrams. Values for g_A^2 and g_V^2 from $\mu^+\mu^-$ pair data and for $\sin^2\theta_W$ from e^+e^- pair data

^c QED radiative corrections for μ pairs include γ and Z exchange diagrams. Values for g_A^2 and g_V^2 from $\mu^+\mu^-$ pair data and for $\sin^2\theta_W$ from combined e^+e^- and $\mu^+\mu^-$ pair data

^d QED radiative corrections for μ pairs include γ and Z exchange diagrams

^e QED radiative corrections for μ pairs include γ and Z exchange diagrams. Values for g_A^2 , g_V^2 and $\sin^2\theta_W$ from combined e^+e^- and $\mu^+\mu^-$ pair data

$e^+e^- \rightarrow \mu^-$

The data sample contains 2673 $\mu^+\mu^-$ events. In the μ pair analysis at least one track was required to be identified as a muon by the muon chambers or the liquid argon calorimeter [5]. Both identification methods gave the same results within statistics. The data were corrected for detector losses and higher order QED effects using the Monte Carlo program of Berends et al. [11]. The radiative corrections include QED contributions to order α^3 for the photon and Z^0 exchange diagrams. For the TASSO acceptance these radiative effects introduce a positive forward-backward charge asymmetry of +0.023. If only QED diagrams (γ exchange) were considered the observed asymmetry would be altered by +0.016. Weak radiative corrections are expected to be smaller* and were not considered. The systematic uncertainty in the measurement contributing to the asymmetry value was estimated to be less than $\pm 0.5\%$. It includes trigger and track reconstruction ($\pm 0.1\%$), background sources ($\pm 0.1\%$) and acceptance calculations ($\pm 0.4\%$), but no uncertainty for radiative corrections. For cross section determinations the systematic errors are $\pm 2.5\%$ from the overall detection efficiency and $\pm 3.0\%$ from luminosity measurement (using small angle and wide angle Bhabha scattering).

The total cross section was used to test QED. Cut-off parameters were introduced through a time-like form factor given by (6). The results are given in Table 2a.

* The weak corrections to the asymmetry were estimated by Wetzel [12] to be +0.002, while Decker et al. [12] estimate -0.006

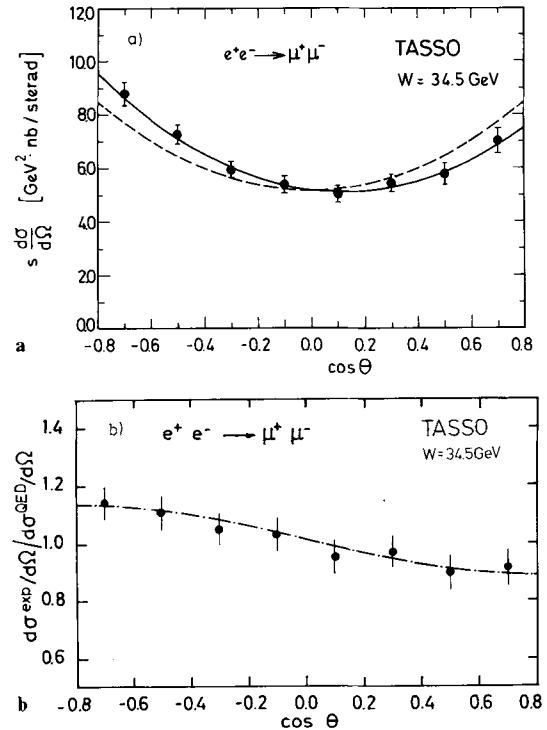


Fig. 2. **a** The differential cross section for the reaction $e^+e^- \rightarrow \mu^+\mu^-$. The dashed line shows the QED expectation, the full line shows the result of the fit with $A_{\mu\mu} = -0.098$. **b** The differential cross section divided by the QED prediction for the reaction $e^+e^- \rightarrow \mu^+\mu^-$. The curve shows the fit to the data of the GWS theory with $\sin^2\theta_W = 0.27$

The differential cross section $s \cdot d\sigma/d\Omega$ is shown in Fig. 2 and listed in Table 3. A clear forward-backward charge asymmetry is observed. Fitting the angular distribution to the form $d\sigma/d\Omega \propto 1 + a \cdot \cos \theta + \cos^2 \theta$

Table 3. Cross section of $e^+e^- \rightarrow \mu^+\mu^-$ at $W=34.5$ GeV. The errors include statistical and systematic uncertainties apart from an overall normalization of $\pm 3.0\%$

$\langle \cos \theta \rangle$	$s \cdot d\sigma/d\Omega$ (GeV ² ·nb/stead)	$\sigma^{\text{meas}}/\sigma^{\text{QED}}$
0.70	7.05 ± 0.43	0.911 ± 0.061
0.50	5.79 ± 0.36	0.891 ± 0.062
0.30	5.43 ± 0.30	0.958 ± 0.055
0.10	5.03 ± 0.29	0.957 ± 0.057
-0.10	5.46 ± 0.31	1.040 ± 0.057
-0.30	6.07 ± 0.32	1.071 ± 0.054
-0.50	7.43 ± 0.40	1.144 ± 0.055
-0.70	8.85 ± 0.50	1.143 ± 0.057

yielded for the asymmetry extrapolated to the full polar angle acceptance*

$$A_{\mu\mu} = \frac{3}{8}a = -0.098 \pm 0.023 \pm 0.005.$$

To first order the asymmetry is related to the axial vector couplings through

$$A_{\mu\mu}^{\text{th}} = -2.7 \cdot 10^{-4} g_A^e \cdot g_A^\mu \cdot \frac{s}{1-s/M_Z^2}. \quad (8)$$

In the standard theory, assuming $M_Z=95$ GeV, one gets $A_{\mu\mu}^{\text{GWS}} = -0.093$ at $W=34.5$ GeV. From the asymmetry measurement we derived the product of the axial vector coupling constants $g_A^e \cdot g_A^\mu = 0.26 \pm 0.06$. Taking $g_A^e = -0.514 \pm 0.058$ from the combined neutrino electron data the axial vector coupling of the muon can be extracted as $g_A^\mu = -0.51 \pm 0.13$. The axial vector couplings for both leptons are the same within errors as expected from $e-\mu$ universality. Using (5) with $I_L = \frac{1}{2}$ and $\rho=1$ one gets $I_{3R} = 0.01 \pm 0.13$. These results are in very good agreement with the GWS theory, which predicts $g_A^\mu = -\frac{1}{2}$ and $I_{3R}^\mu = 0$. Within the GWS theory a one parameter fit gives $\sin^2 \theta_W = 0.26 \pm 0.10$. Results of fits to determine the electroweak parameters are given in Table 2a. They are in good agreement with results obtained from other experiments (Table 2b).

Combined Analysis of e^+e^- and $\mu^+\mu^-$ Pairs

Assuming lepton universality a combined analysis of $e^+e^- \rightarrow e^+e^-$ and $e^+e^- \rightarrow \mu^+\mu^-$ was performed. Since the two reactions have different sensitivities to the weak coupling constants, the combined analysis leads to improved results.

* Compared to our previous publication [5] the measured asymmetry decreased by about 2 s.d. This change is consistent with statistical fluctuations; no change in the detector response has been observed

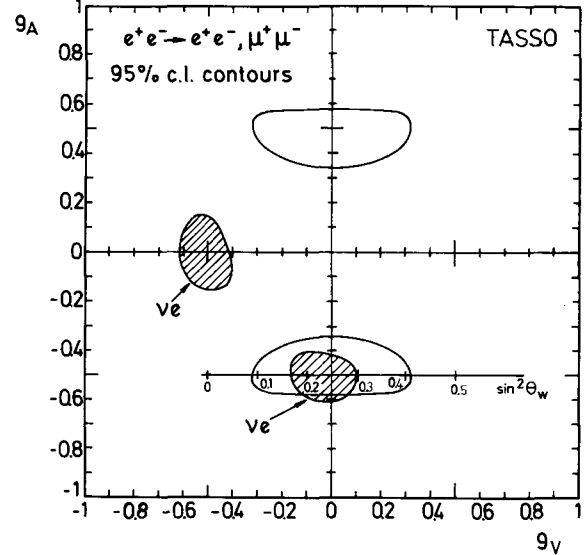


Fig. 3. Results of a fit to g_V and g_A with 95% c.l. contours. The shaded areas show the two solutions from ve experiments

The results of fits to the different assumptions (i)–(iii) are summarized in Table 2a. The data are well described by the standard theory yielding a value of $\sin^2 \theta_W = 0.27 \pm 0.07$. In Figs. 1 and 2b a fit to the differential cross sections is shown for $\sin^2 \theta_W = 0.27$. The determination of g_V and g_A leads to two solutions. They are displayed in the g_V-g_A plane of Fig. 3 together with the combined neutrino electron scattering data. Using the neutrino data to resolve the sign ambiguity we obtain $g_V = 0.000 \pm 0.170$ and $g_A = -0.481 \pm 0.055$. The agreement between our results and the ve data is good although the squared momentum transfers differ by more than four orders of magnitude viz. $Q^2(ve) < 0.1$ GeV² and $Q^2(e^+e^-) > 10^3$ GeV². For the right-handed isospin assignment we find $I_{3R} = -0.019 \pm 0.055$, a value well compatible with zero. Taking $I_{3R} = 0$ and $I_{3L} = -1/2$ we obtain $\rho = 0.93 \pm 0.22$ from (5).

These results are in excellent agreement with the GWS theory, which predicts $g_V = -0.04$ (for $\sin^2 \theta_W = 0.23$) and $g_A = -\frac{1}{2}$ and assumes the leptons to be grouped in left-handed doublets ($I_L = \frac{1}{2}$) and right-handed singlets ($I_R = 0$). Assuming the standard theory and $\sin^2 \theta_W = 0.23$ an upper limit on the parameter c was found to be $c < 0.013$ (95% c.l.).

Our results are in good agreement with other e^+e^- experiments. In Table 2b they are compared with recent measurements of electroweak parameters.

Test of Composite Models

In many models the fundamental fermions are supposed to be composite structures. The authors of [13] have proposed a general parametrization of

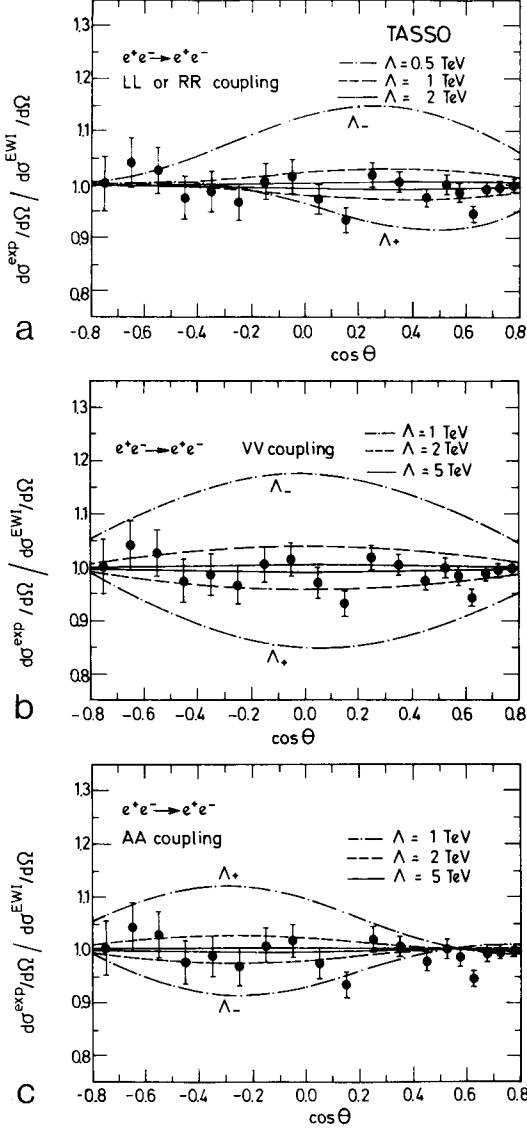


Fig. 4a-c. The differential cross section divided by the prediction of the standard theory for the reaction $e^+e^- \rightarrow e^+e^-$. The curves show possible contributions from composite models for **a** left-handed or right-handed coupling, **b** vector coupling and **c** axial vector coupling

substructures, which does not depend on a specific model. They assume the validity of the standard electroweak theory and add to its lagrangian a point-like interaction of the form

$$L_{\text{eff}} = \pm \frac{g^2}{2\Lambda_{\pm}^2} \{ \eta_{LL} j_L \cdot j_L + \eta_{RR} j_R \cdot j_R + 2\eta_{RL} j_R \cdot j_L \}. \quad (9)$$

The parameter Λ characterizes the mass scale of compositeness and is defined such that $g^2/4\pi=1$. The overall sign of the interaction is indicated by the subscripts \pm of the parameter Λ . j_L and j_R are left- and right-handed currents and the coefficients η

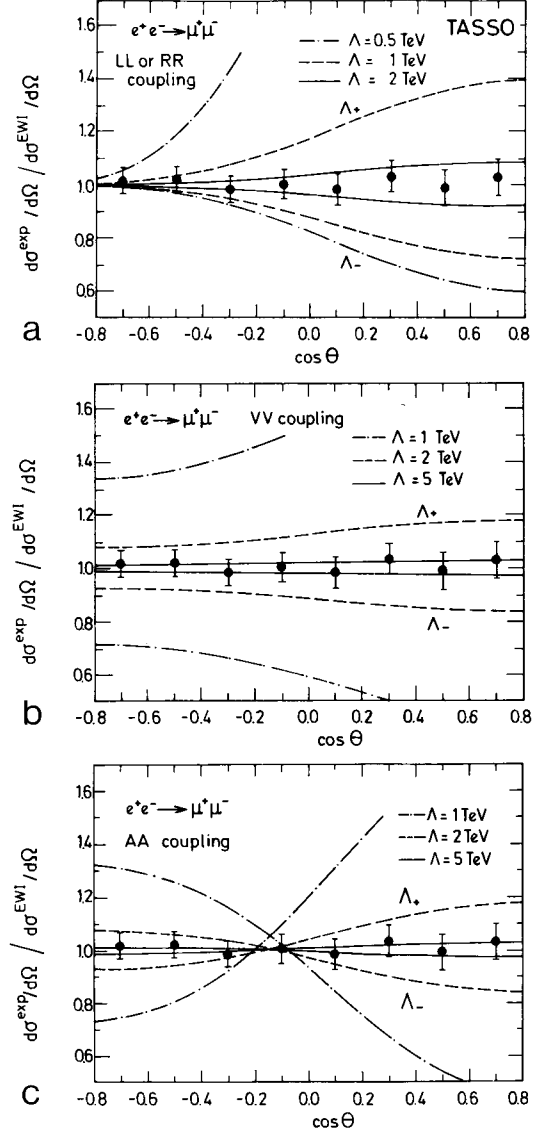


Fig. 5a-c. The differential cross section divided by the prediction of the standard theory for the reaction $e^+e^- \rightarrow \mu^+\mu^-$. The curves show possible contributions from composite models for **a** left-handed or right-handed coupling, **b** vector coupling and **c** axial vector coupling

take only values of either 0 or ± 1 (e.g. $\eta_{LL}=1$, $\eta_{RR}=\eta_{RL}=0$ for LL coupling or $\eta_{LL}=\eta_{RR}=\eta_{RL}=1$ for VV coupling). Interference with the standard processes (γ and Z^0 exchange) would result in deviations in the angular distributions. In the case of Bhabha scattering the constituents are the same in the initial and final states. For μ pair production such an interaction requires e and μ to have common constituents, and is therefore less general. To analyse the data in terms of the lagrangian of (9) the effects of the electroweak interference were first divided out assuming the standard theory with $\sin^2\theta_W$

Table 4. Lower limits (95% c.l.) on A_{\pm} parameters in composite models for left-handed (L), right-handed (R), vector (V) and axial vector (A) couplings

Coupling	$e^+e^- \rightarrow e^+e^-$		$e^+e^- \rightarrow \mu^+\mu^-$	
	A_+	A_-	A_+	A_-
LL	0.70 TeV	1.94 TeV	2.13 TeV	2.65 TeV
RR	0.70 TeV	1.94 TeV	2.11 TeV	2.62 TeV
VV	1.86 TeV	2.91 TeV	3.43 TeV	4.37 TeV
AA	1.95 TeV	2.28 TeV	3.05 TeV	3.40 TeV

=0.23. In Figs. 4 and 5 we show the sensitivity of the Bhabha and μ pair data to several values of A and different couplings of left-handed (L), right-handed (R), vector (V) and axial vector (A) currents. Lower limits on the parameters A_+ and A_- are given in Table 4. They are of the order of 1–4 TeV and are typically an order of magnitude larger than those obtained in the conventional QED cut-off analysis described above. Note, however, that the A values obtained are directly related to the assumed coupling strength $g^2/4\pi$. Note also that at present energies LL and RR couplings are indistinguishable.

Summary

In conclusion the analysis of the reactions $e^+e^- \rightarrow e^+e^-$ and $e^+e^- \rightarrow \mu^+\mu^-$ at a c.m. energy of 34.5 GeV has lead to improved results on the leptonic electroweak coupling constants. The results are in agreement with other e^+e^- experiments at PETRA and PEP [7] and with low energy neutrino electron scattering experiments [4]. They confirm the standard theory predictions and complement the W^{\pm} and Z^0 discoveries [8, 9] in fixing the leptonic couplings. Limits have been put on the mass scale for a certain class of composite models.

Acknowledgements. We thank our technicians for their continuous effort to maintain the detector. Those of us from abroad wish to thank the DESY directorate for the hospitality extended to us while working at DESY.

Appendix

In this section a short summary on the data analysis for the reactions $e^+e^- \rightarrow e^+e^-$ and $e^+e^- \rightarrow \mu^+\mu^-$ will be given. More details can be found in [5, 6, 14, 15]. Both analyses have many common aspects, therefore they will be described in parallel as much as possible.

Event Selection Criteria

The selection of two prong events proceeded through the following cuts:

	$e^+e^- \rightarrow e^+e^-$	$e^+e^- \rightarrow \mu^+\mu^-$
a) Selection of two oppositely charged tracks		
b) Acollinearity angle	$\xi < 10^\circ$	
c) Polar angle	$ \cos \theta < 0.80$	
d) Momentum	$P > 0.2 p_{\text{beam}}$	$P > 0.5 p_{\text{beam}}$
	$\Sigma p > 0.7 p_{\text{beam}}$	
e) Vertex restriction		
\perp beam	$ d_0 < 0.6$ cm	$ d_0 < 0.4$ cm
\parallel beam	$ z < 7.5$ cm	$ z < 4.0$ cm
f) Time of flight	$-3.0 < t^{\text{meas}} - t^{\text{pred}} < 2.0$ ns	

For the Bhabha event analysis no electron identification was required. In this data sample background from two-photon processes $e^+e^- \rightarrow e^+e^-l^+l^-$ and cosmic rays is negligible. The contribution from μ pairs (5% overall and 20% in the backward hemisphere) and τ pairs (1%) was subtracted bin by bin taking our measured angular asymmetry into account.

Events were classified as μ pairs if at least one track

(i) penetrated the iron absorber and had associated hits in ≥ 3 out of 4 muon chambers or (ii) deposited less than 1.5 GeV shower energy in a single cluster in the liquid argon calorimeter and no other close-by cluster was detected.

The two identification methods were cross checked against each other. Backgrounds from $e^+e^- \rightarrow e^+e^- \mu^+\mu^-$ and $e^+e^- \rightarrow e^+e^-$ were found to be negligible; the background from cosmic rays amounted to 0.3% while τ pairs yielded a background of 2.0%.

Efficiencies and Resolutions

The trigger and reconstruction efficiency as well as the efficiency of the different detector components were checked with data taken concurrently with other independent triggers. The efficiencies were determined with a typical accuracy of $\pm 1\%$ and, most important, did not show any polar angle dependence on the charge of the tracks.

The following apparatus effects limiting the accuracy of the asymmetry measurement were considered:

(1) Asymmetries due to trigger and track reconstruction were studied with multihadron events,

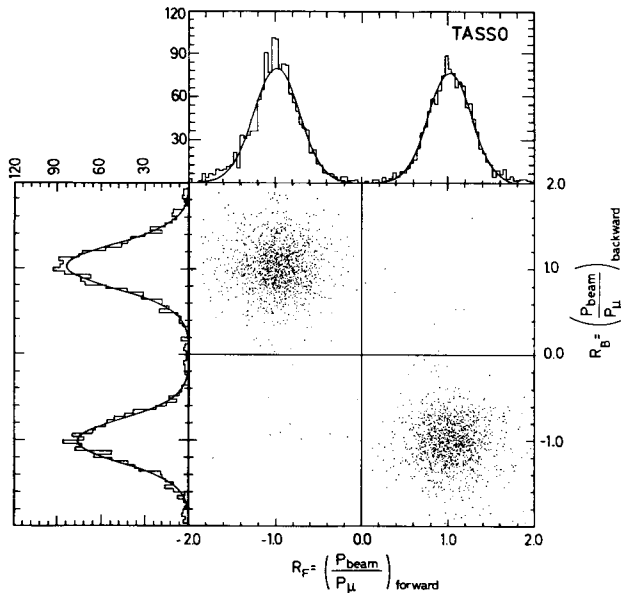


Fig. 6. The normalized reciprocal momentum $R = p_{\text{beam}}/p$ plotted for forward (R_F) and backward (R_B) muons in the reaction $e^+e^- \rightarrow \mu^+\mu^-$ at $\sqrt{s} = 34.5$ GeV. The sign of R is the charge determined from the track curvature

two-photon events $e^+e^- \rightarrow e^+e^-\mu^+\mu^-$ and cosmic rays. Within our statistics no forward-backward asymmetry was observed at a level of 1%.

(2) Poor momentum measurement or a twist of the central drift chamber could lead to a wrong charge assignment for both tracks simultaneously. To control this effect we studied the correlations of the charge weighted reciprocal momenta of forward versus backward going muons [5]. The distribution of 2690 μ pairs shown in Fig. 6 contains $7\mu^+\mu^+$ and $10\mu^-\mu^-$ pairs. This leads to a charge confusion probability of $(0.3 \pm 0.1)\%$ per track. From the density around the origin the correlated charge flip probability was estimated to be less than 10^{-5} . This implies that the curvature measurements of the two tracks are independent from each other. These numbers are also consistent with those derived from the momentum resolution $\sigma_p/p = 0.016 \cdot p_t$ (p in GeV/c).

Acceptance Calculations

The acceptance functions used to correct the measured angular distributions were calculated by Monte Carlo using the event generators of Berends et al. [16]. Electrons were simulated with the EGS code [17] and good agreement with the data was obtained. We estimate the overall uncertainty due to shower corrections in the bin-to-bin polar angle acceptance to be less than 1%. Muon tracks were projected into the muon chambers and liquid argon

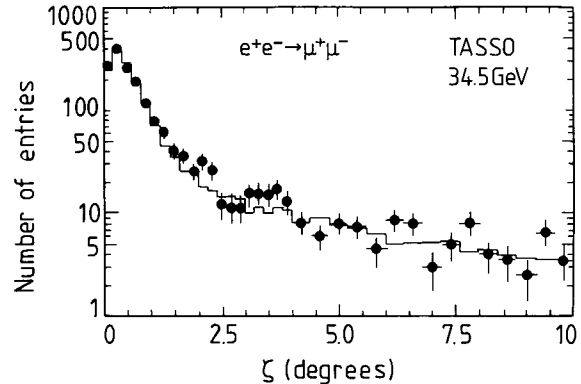


Fig. 7. The observed acollinearity distribution for the reaction $e^+e^- \rightarrow \mu^+\mu^-$. The histogram shows the QED prediction including radiative corrections up to order α^3

calorimeter taking all detector effects into account. The acceptance is a rapidly varying function in the polar angle range $0.5 < |\cos \theta| < 0.8$. Different procedures for calculating the acceptance were used; they produce a maximum change in the asymmetry of $\pm 0.4\%$. Higher order QED processes induce angular asymmetries which are dependent on the experimental selection criteria. Radiative corrections up to order α^3 were calculated as described in the text and were found to agree well with the experimental data. As an example we show in Fig. 7 the μ pair acollinearity distribution.

Cross Section Formula

The cross sections were evaluated using the formula of [18] for the electroweak interaction and extended by the authors of [13] for composite models. For Bhabha scattering with unpolarized beams the cross section can be written in the following form

$$\frac{d\sigma}{d\Omega} = \frac{\alpha^2}{8s} \{4B_1 + B_2(1 - \cos \theta)^2 + B_3(1 + \cos \theta)^2\} \quad (\text{A1})$$

with

$$B_1 = \left(\frac{s}{t}\right)^2 \left| 1 + (g_V^2 - g_A^2) \xi + \frac{\eta_{RL} \cdot t}{\alpha \Lambda^2} \right|^2,$$

$$B_2 = \left| 1 + (g_V^2 - g_A^2) \chi + \frac{\eta_{RL} \cdot s}{\alpha \Lambda^2} \right|^2,$$

$$B_3 = \frac{1}{2} \left| 1 + \frac{s}{t} + (g_V + g_A)^2 \left(\frac{s}{t} \xi + \chi \right) + \frac{2\eta_{RR} s}{\alpha \Lambda^2} \right|^2 \\ + \frac{1}{2} \left| 1 + \frac{s}{t} + (g_V - g_A)^2 \left(\frac{s}{t} \xi + \chi \right) + \frac{2\eta_{LL} s}{\alpha \Lambda^2} \right|^2,$$

$$\chi = \frac{G_F \cdot M_Z^2}{2\sqrt{2}\pi\alpha} \cdot \frac{s}{s - M_Z^2 + iM_Z\Gamma},$$

$$\xi = \frac{G_F \cdot M_Z^2}{2\sqrt{2}\pi\alpha} \cdot \frac{t}{t - M_Z^2 + iM_Z\Gamma}.$$

G_F is the Fermi constant, M_Z and Γ the mass and width of the Z^0 boson. In the GWS theory the weak couplings are given by $g_V = -\frac{1}{2}(1-4\sin^2\theta_W)$ and $g_A = -\frac{1}{2}$. Extended models can be described by replacing g_V^2 by $g_V^2 + 4c$. Composite models are tested by allowing some of the coefficients η to be unequal to zero and the mass scale Λ to be finite. From formula (A1) the cross section for μ pair production can easily be derived by setting all terms with s/t to zero.

References

1. S.L. Glashow: Nucl. Phys. **22**, 579 (1961); S. Weinberg: Phys. Rev. Lett. **19**, 1264 (1967); A. Salam: Proc. eighth Nobel Symp., p.367. Ed. N. Svartholm. Stockholm: Almquist and Wiksell 1968
2. P.Q. Hung, J.J. Sakurai: Nucl. Phys. **B143**, 82 (1978); J.D. Bjorken: Phys. Rev. **D19**, 335 (1979); E.H. de Groot et al.: Phys. Lett. **90B**, 427 (1980); **95B**, 128 (1980); V. Barger et al.: Phys. Rev. Lett. **44**, 1169 (1980); Phys. Rev. **D22**, 727 (1980)
3. P. Fayet: Proc. XXI Int. Conf. on High Energy Physics, Paris, 1982, J. Phys. (Paris) Suppl. **43**, C3-673 (1982); R. Kögerler: Electroweak interactions at high energies. Proc. 1982 DESY Workshop, eds. R. Kögerler, D. Schildknecht, Singapore: World Scientific Publications 1983
4. Recent compilations of electroweak parameters can be found in: J.E. Kim, P. Langacker, M. Levine, H. Williams: Rev. Mod. Phys. **53**, 211 (1981); Particle Data Group: Phys. Lett. **112B**, 1 (1982); M. Davier: Rapporteur's talk at XXI Int. Conf. High Energy Physics, Paris, 1982; J. Phys. (Paris) Suppl. **43**, C3-471 (1982); W. Krenz: RWTH Aachen preprint, PITHA 82/26
5. TASSO Collab. R. Brandelik et al.: Phys. Lett. **110B**, 173 (1982)
6. TASSO Collab. R. Brandelik et al.: Phys. Lett. **117B**, 365 (1982)
7. CELLO Collab. H.J. Behrend et al.: Z. Phys. C - Particles and Fields **14**, 283 (1982); Phys. Lett. **103B**, 148 (1981); JADE Collab. W. Bartel et al.: Phys. Lett. **108B**, 140 (1982); DESY Report 83-035 (1983); MARK-J Collab. B. Adeva et al.: Phys. Rev. Lett. **48**, 1701 (1982); PLUTO Collab. Ch. Berger et al.: DESY Report 83-084 (1983); MAC Collab. E. Fernandez et al.: Phys. Rev. Lett. **50**, 1238 (1983)
8. UA1 Collab. G. Arnison et al.: Phys. Lett. **122B**, 103 (1983); UA2 Collab. G. Banner et al.: Phys. Lett. **122B**, 476 (1983)
9. UA1 Collab. G. Arnison et al.: Phys. Lett. **126B**, 398 (1983); UA2 Collab. P. Bagnaia et al.: Phys. Lett. **129B**, 130 (1983)
10. F.A. Berends, K.J.F. Gaemers, R. Gastmans: Nucl. Phys. **B63**, 381 (1973); **B68**, 541 (1974); F.A. Berends, G.J. Komen: Phys. Lett. **63B**, 432 (1976); F.A. Berends, R. Gastmans: Nucl. Phys. **B61**, 414 (1973); F.A. Berends, R. Kleiss: Inst. Lorentz, Leiden, preprint, July 1983
11. F.A. Berends, R. Kleiss, S. Jadach: Nucl. Phys. **B202**, 63 (1982); M. Böhm, W. Hollik: DESY 83-060
12. W. Wetzel: Heidelberg University preprint, May 1983; R. Decker, E.A. Paschos, R.W. Brown: Dortmund University preprint, DO-TH 83/16
13. E.J. Eichten, K.D. Lane, M.E. Peskin: Phys. Rev. Lett. **50**, 811 (1983)
14. H. Burkhardt: Thesis, Univ. Hamburg, 1982, DESY F35-82-03
15. M. Ogg: Ph.D. Thesis, Univ. Oxford, 1981; RL-HEP-T-89; I.C. Brock: Ph.D. Thesis, Univ. Oxford, 1983; RL-HEP-T-106
16. F.A. Berends, R. Kleiss: Nucl. Phys. **B177**, 237 (1981); F.A. Berends, R. Kleiss, S. Jadach: Nucl. Phys. **B202**, 63 (1982); F.A. Berends, R. Kleiss: Inst. Lorentz, Leiden, preprint, July 1983
17. R.L. Ford, W.R. Nelson: EGS Code, SLAC-210 (1978)
18. R. Budny: Phys. Lett. **55B**, 227 (1975)